Available online at www.sciencedirect.com

ScienceDirect

Transportation Research Procedia 72 (2023) 224–231

Transportation Research Procedia

www.elsevier.com/locate/procedia

Transport Research Arena (TRA) Conference

URANS prediction of ship performance: An analysis of propulsion system failure on turning behaviour of a ship in waves

Daejeong Kim[a]*, Claire DeMarco Muscat-Fenech[b], Yigit Kemal Demirel[a] and Tahsin Tezdogan[a]

[a]*Department of Naval Architecture, Ocean and Marine Engineering, University of Strathclyde, 100 Montrose Street, Glasgow G4 0LZ, United Kingdom*

[b]*Department of Mechanical Engineering, Faculty of Engineering, University of Malta, MSD2080, Msida , Malta*

Abstract

The loss of ship propulsive power has been recognised as the most frequently occurring incident at sea. Given the fact that the manoeuvrability of a ship is highly reliant on the propulsive power produced by a rotating propeller, propulsion loss may pose potential threats to navigational safety in a real seaway by resulting in further serious incidents, such as collision, contact, and grounding. The key objective of this paper is to analyse the propulsion loss impacts on the turning capability of the KRISO Container Ship (KCS) model in different wave height conditions, using unsteady Reynolds-Averaged Navier-Stokes (URANS) computations. It is expected that this work will be of great interest to Master Mariners and navigating officers who are in charge of ship handling and help enhance navigational safety in real sea states.

Keywords: Ship manoeuvrability; seakeeping; turning capability; computational fluid dynamics (CFD); propulsion loss

1. Introduction

The European Maritime Safety Agency (EMSA) has investigated marine casualties and incidents over the period between 2014 and 2020 (EMSA, 2021). According to the accident investigation report, the loss of ship propulsive power has been recognised as the most frequently occurring incident at sea, as presented in Fig. 1. It is also reported that the incidence of propulsion failure events largely increased over the past few years. Hasnan et al. (2019) demonstrated that the manoeuvring performance of a ship is highly reliant on the propulsive power induced by a rotating propeller, which may be decisive in determining the rudder normal force directly affecting the steering ability.

* Corresponding author. Tel.: +01-4154-8453.
E-mail address: daejeong.kim@strath.ac.uk

10.1016/j.trpro.2023.11.398

Given this, it is thought that propulsion loss may pose potential threats to navigational safety in a real seaway by resulting in further serious incidents, such as collision, contact, and grounding due to the lack of adequate steering. An in-depth understanding of the manoeuvring behaviour of a ship with propulsion system failure is therefore necessary for proper decision-making about ship handling and consequently navigational safety at sea. The main aim of this paper is to investigate the contribution of the propulsion loss to the manoeuvrability of a ship in different wave conditions.

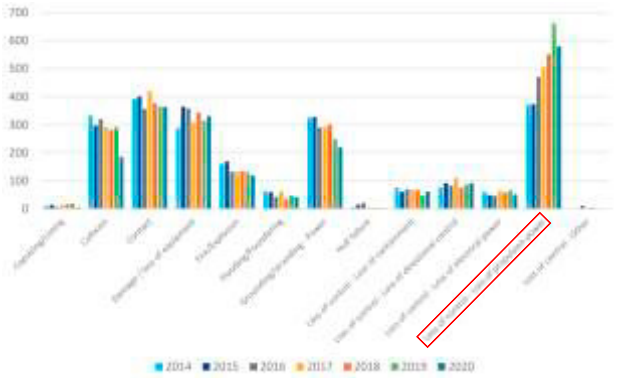

Fig. 1. Distribution of casualty events with a ship over the period 2014-2019, adapted from EMSA (2021).

In general, there are several approaches to estimate the manoeuvring performance of a ship: theoretical methods, experimental methods, and Computational Fluid Dynamics (CFD) based methods. Among these approaches, free-running simulations by means of an unsteady Reynolds Averaged Navier-Stokes (URANS) solver are increasingly gaining popularity as the state-of-the-art tool applicable to ship manoeuvring problems with advances in computational processing power and numerical algorithms (ITTC, 2021). The major advantages of the free-running CFD simulation lie in its capability in accounting for viscous and turbulent effects being significant on ship manoeuvring and in providing very detailed results related to hydrodynamic loads, surface elevations, and velocity/pressure fields experienced by a manoeuvring ship. Broglia et al. (2015), for example, performed the free-running CFD simulation to investigate the turning capability of a naval supply vessel in calm water by means of an unsteady RANS solver. To model the flow field interaction between the hull, the propellers and the rudder, an actuator disk model properly modified to take into account oblique flow effects was adopted for the free-running CFD model. The numerical results obtained from their study consisting of kinematic and dynamic parameters during the manoeuvre were compared to free-running model tests and showed a good agreement. In Wang et al. (2016), URANS simulations for the ONR Tumblehome ship model performing 6DOF self-propulsion and turning circle manoeuvres in calm water were described. The work states that the propeller was directly discretised, such that the strict requirements for the resolution of the propeller flow should be complied with. By comparison with available experimental results, the validity of the free-running CFD simulations has been proved. The comparison in terms of both trajectory and kinematic parameters showed an overall agreement. Kim et al. (2021d) investigated the manoeuvrability of the KVLCC2 performing turning and zigzag manoeuvres in calm water. Kim et al. (2021d) used the CFD software STAR-CCM+, as a RANS solver, to carry out free-running simulations. Their research demonstrated the effectiveness of the free-running CFD simulation to predict the manoeuvrability of a ship, with satisfactory comparisons between the CFD results and experiments. It is worth introducing recent studies where free-running simulations were carried out to predict the manoeuvrability of a ship in waves by means of a fully unsteady RANS solver: Kim et al. (2021a); Kim et al. (2021b); Kim et al. (2021c); Kim et al. (2022); Kim and Tezdogan (2022). Given the benefits of free-running CFD simulations, this paper is based on the CFD-based unsteady RANS simulations of ship manoeuvres and seakeeping performance in waves. This can be tackled by conducting unsteady Reynolds-Averaged Navier-Stokes computations coupled with the equations of rigid body motion with full six degrees of freedom.

Considerable research published in the field of ship manoeuvrability has been devoted to the investigation of a ship's manoeuvrability in normal operating conditions where all machinery pertaining to the navigation system is in

proper working conditions. However, their findings may be inconclusive on a vital question regarding the manoeuvring performance of a ship experiencing a failed propulsion system in a real seaway. Although the authors' previous study (Kim et al., 2022) evaluated the effects of a propulsion failure on the manoeuvrability of a ship in regular waves of different directions, it is thought that more various wave conditions should be further applied for the follow-up study. In this context, this paper was motivated to investigate the effects of the propulsion loss on the manoeuvrability of a ship under different wave height conditions.

The work presented here is organised as follows: Section 2 presents the methodology adopted in this work, along with a list of the simulation cases to which the current CFD model is applied and a brief description of the numerical setup for the model. Afterwards, the CFD results obtained from the simulations are provided in Section 3. Finally, concluding observations are given in Section 4.

2. Methodology

The section will outline the research methodology adopted in this paper, with a brief description of the numerical setup for the current CFD model. Fig. 2 presents the research methodology used in this study, consisting of four main steps to investigate the effects of a propulsion failure on a ship's manoeuvrability using CFD: *1) goal and scope, 2) numerical modelling, 3) execution of free running simulations, and 4) results of analysis*.

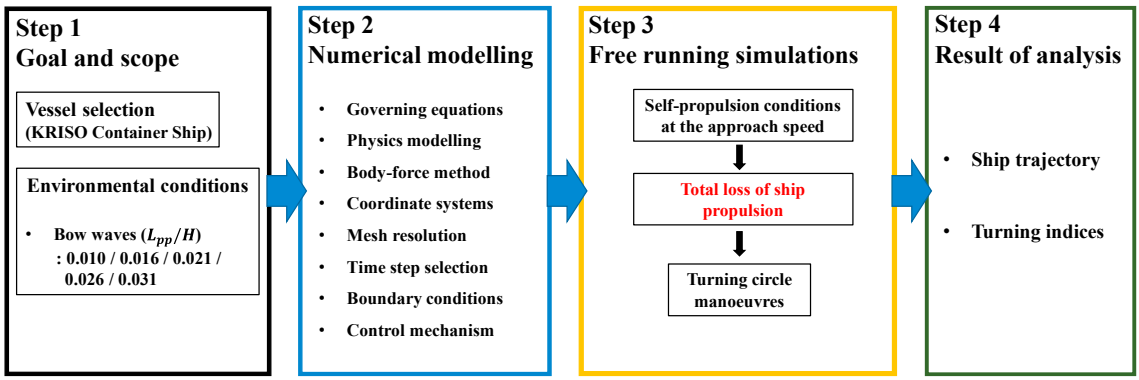

Fig. 2. Research methodology applied to the CFD free-running simulations.

2.1. Goal and scope

All the numerical simulations were performed for the KCS model with a scale factor of 75.24, and the main properties of the ship are listed in Table 1.

Table 1. Principal particulars of the KCS.

Main particulars	Symbols	Model scale (1:75.24)
Length between the perpendiculars	L_{BP} (m)	3.057
Length of waterline	L_{WL} (m)	3.0901
Beam at waterline	$B_{W.L}$ (m)	0.4280
Draft	D (m)	0.1435
Displacement	Δ (m^3)	0.1222
Block coefficient	C_B	0.651
Ship wetted area with rudder	S (m^2)	1.6834
Longitudinal centre of buoyancy	% $L_{BP,}$ fwd+	-1.48
The metacentric height	GM (m)	0.008
Radius of gyration	K_{xx}/B	0.49
Radius of gyration	K_{yy}/L_{BP}, K_{zz}/L_{BP}	0.25
Propeller diameter	D_P (m)	0.105
Propeller rotation direction (view from stern)		Clockwise
Rudder turn rate	(deg./s)	20.1

A series of turning manoeuvres experienced by the ship with propulsion system failure were carried out in bow waves with the wave heights H = 0.032m, 0.048m, 0.064m, 0.080m, and 0.096m, corresponding to H=2.4m, 3.6m, 4.8m, 6.0m, and 7.2m in full-scale, respectively. The cases to be simulated in CFD are presented in Table 2 and Fig. 3.

Table 2. The self-propulsion simulation cases to which the CFD model is applied prior to the turning circle manoeuvres in the propulsion failure.

Case no.	Approach speed U_0 (m/s)	Propeller rev. (RPS)	Wave height H (m)	Encounter Angle μ (degrees)	Encounter Period T_e (s)	Wave steepness H/ λ	Wave/ship length λ/L_{BP}
1	1.004	13.38	0.032	225 (Bow sea)	1.055	0.010	1.00
2	0.945	13.38	0.048	225 (Bow sea)	1.071	0.016	1.00
3	0.876	13.38	0.064	225 (Bow sea)	1.087	0.021	1.00
4	0.811	13.38	0.080	225 (Bow sea)	1.104	0.026	1.00
5	0.737	13.38	0.096	225 (Bow sea)	1.123	0.031	1.00
6	1.094	13.38	Calm water	- (Calm sea)	-	-	-

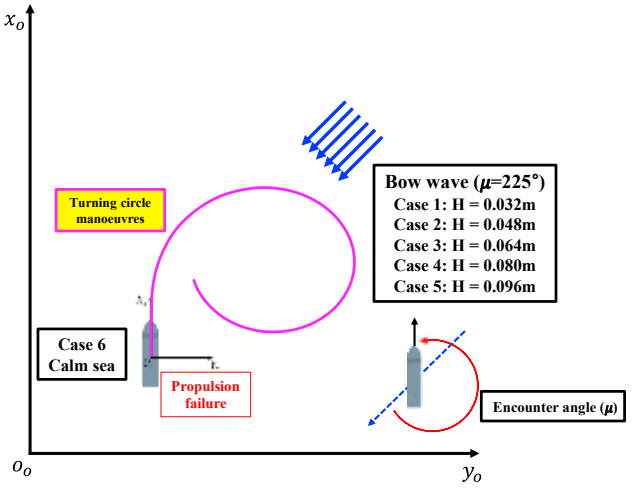

Fig. 3. The schematic view of the simulation cases applied to this study.

It is important to mention that the self-propulsion condition should be first attained before performing turning manoeuvres in the propulsion failure condition. Throughout all the self-propulsion computations, the propeller revolution rate was set at 13.38 n/sec (*n* is the rotational speed of the propeller in RPS (revolutions per second)). It can be seen from Table 2 that the approach speed of the ship was different for each case, stemming from the difference in added resistance depending on the wave height applied. The turning manoeuvres of the ship suffering from propulsion loss were performed from the stable state of self-propulsion condition, executing a propeller speed controller which acts on the propeller rotational speed and a rudder angle controller for the turning manoeuvre. In this study, the rotating propeller was designed to stop suddenly as the ship started the turning manoeuvre to represent the propulsion loss condition (from 13.38 n/sec to 0 n/sec according to the propeller controller).

2.2. Numerical modelling

In this work, the free-running simulations were carried out using the commercial CFD package STAR-CCM+, version 15.04. The main features of the numerical modelling and computational schemes for the free-running CFD model are only briefly recalled here; for detailed information reference can be made to Kim et al. (2021a); Kim et al. (2021b); Kim et al. (2021c); Kim et al. (2022), and Kim and Tezdogan (2022).

The CFD code adopted in this study solves the unsteady Reynolds Averaged Navier-Stokes (URANS) equations for turbulent flows around the ship performing a self-propelled manoeuvre. The solver is based on a finite volume method which discretises the governing equations, using the Menter's Shear Stress Transport (SST) model (Menter,

1994) for the closure of the system. The SIMPLE algorithm was employed for pressure-velocity coupling in the numerical simulation. In order to simulate the multiphase flow of air and water, the Volume of Fluid (VOF) method was used. The rotating propeller effects during ship manoeuvres were simulated by means of an actuator disk model based on the body force method, where both axial and tangential body forces are distributed in the flow field within the actuator disk of finite thickness. The fifth-order Stokes wave model was adopted to generate non-linear regular waves in the free-running simulations. As can be found in the authors' previous work (Kim et al., 2021c), four different frames of reference were used for the free-running CFD model: *(1) Earth-fixed coordinate ($o_o - x_oy_oz_o$), (2) Ship-fixed coordinate (o_s - $x_sy_sz_s$), 3) Propeller-fixed coordinate (o_p - $x_py_pz_p$), and (4) Rudder-fixed coordinate (o_r - $x_ry_rz_r$).* The Dynamic Fluid Body Interaction (DFBI) module was used to simulate the realistic motion of the ship performing manoeuvres in waves, as presented in Terziev et al. (2020).

In this study, grid generations were carried out by means of the built-in meshing facility in STAR-CCM+, resulting in a computation mesh of approximately 7.2 million cells (Cases 1-5) and 5.4 million cells (Case 6) in total. The computational domain was decomposed in three regions: *1) background region, 2) hull overset region, and 3) rudder blade overset region*. A dynamic overlapping grid approach was used to handle large ship motions and rudder movement during free-running manoeuvres. The computational domain dimensions and the imposed boundary conditions are depicted in Fig. 4.

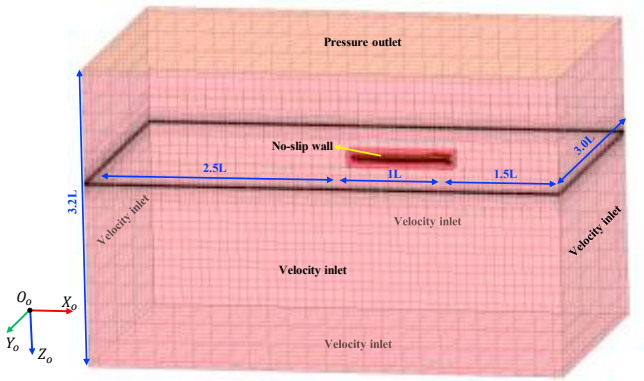

Fig. 4. Domain dimensions and boundary conditions.

3. Results

The turning manoeuvres of the ship with propulsion system failure were simulated based on the methodology shown in Section 2. A series of validation and verification studies for similar problems have been performed by Kim et al. (2021c), presenting promising results. In this section, the results are presented for both the normal and propulsion loss conditions. The details of the ship's turning performance in the normal operating conditions are reported in Kim et al. (2021b). The same simulation duration was used for each case of both conditions (i.e., the normal and propulsion loss conditions) so that the contribution of the propulsion failure to the turning performance is comparable. It has to be stated that the turning manoeuvre with only the yaw angle variation of 360º was considered in the normal conditions due to the high computational cost.

Fig. 5 displays the predicted ship trajectories of the turning manoeuvres for all cases under the normal and propulsion failure conditions. The propulsion loss led to substantial changes in the turning trajectories when compared to those in the normal conditions, clearly evidenced in Fig. 5. It should be emphasised that higher wave heights can cause larger changes in the turning trajectory when the ship lost its propulsion power, in comparison with the normal conditions. As it can be inferred from the figure, the ship suffering from propulsion loss could not complete the turning circle manoeuvre for all cases, mainly due to the reduced inflow velocity to the rudder after the propulsion failure and thus the insufficient rudder normal force.

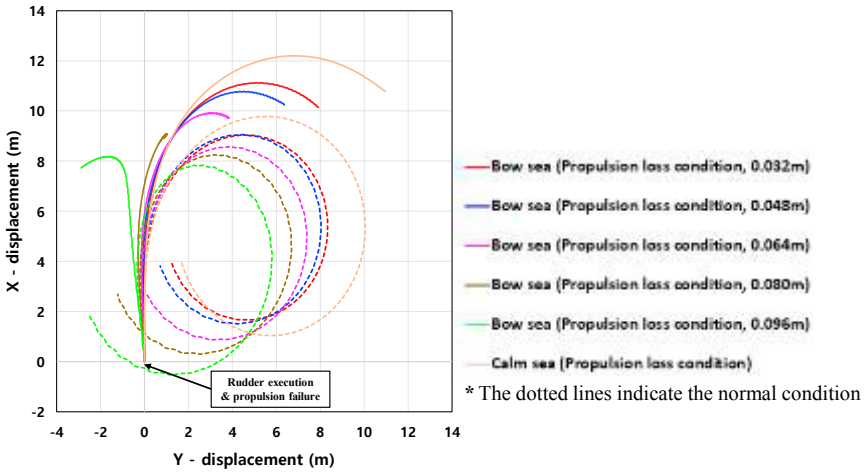

Fig. 5. The turning trajectories in both normal condition and propulsion loss condition.

In Table 3, the important turning parameters (i.e., the advance, the transfer, the tactical diameter, and the time to 90°/180° yaw angle change) are reported. Fig. 6 presents the time histories of the ship's horizontal velocities (i.e., surge, sway, and yaw velocities) during the turning manoeuvre. The ship advance appeared to be larger when the ship lost its propulsion than the normal operating conditions. In addition, it was seen that the advance experienced by the ship was observed to decrease with an increase in the wave height under both normal and propulsion loss conditions. The transfer showed a similar trend too. This is closely associated with the ship's horizontal velocities; in general, the greater the surge speed and the smaller the yaw velocity, the greater the advance and transfer can be. It can be seen that the time taken for 90° turn became significantly longer when compared to the normal condition, due to the insufficient propulsive power (i.e., the rudder normal force). Interestingly, a 180º turn could not be attained for Cases 1 - 4 (propulsion loss conditions), while a 90º turn could not even be achieved in Case 5 (propulsion loss condition). From Fig. 6, it clearly appeared that the propulsion loss noticeably affected the speed loss during the turning manoeuvre when compared to that experienced by the turning ship under the normal conditions. This represents the poor manoeuvring performance of the ship in the propulsion loss condition.

Table 3. CFD results: turning indices in the normal operating and propulsion failure conditions.

Parameters (CFD results)	Bow sea (0.032m) (Case1)	Bow sea (0.048m) (Case 2)	Bow sea (0.064m) (Case 3)	Bow sea (0.080m) (Case 4)	Bow sea (0.096m) (Case 5)	Calm sea (Case 6)
			Normal operating conditions			
Advance (m)	8.79 (2.88 L_{BP})	8.83 (2.89 L_{BP})	8.35 (2.73 L_{BP})	8.04 (2.63 L_{BP})	7.70 (2.52 L_{BP})	9.55 (3.13 L_{BP})
Transfer (m)	3.24 (1.05 L_{BP})	3.09 (1.01 L_{BP})	2.68 (0.88L_{BP})	2.24 (0.73 L_{BP})	1.17 (0.38 L_{BP})	4.07 (1.33 L_{BP})
Time for yaw 90° (s)	12.18	13.08	13.44	14.18	15.10	12.31
Tactical diameter (m)	8.09 (2.65 L_{BP})	7.82 (2.56 L_{BP})	7.17 (2.35L_{BP})	6.54 (2.14 L_{BP})	5.63 (1.84 L_{BP})	9.82 (3.21 L_{BP})
Time for yaw 180° (s)	23.19	24.38	24.93	26.26	27.31	24.20
			Propulsion failure conditions			
Advance (m)	10.83 (3.54 L_{BP})	10.50 (3.43 L_{BP})	9.73 (3.18 L_{BP})	9.03 (2.96 L_{BP})	-	11.87 (3.88 L_{BP})
Transfer (m)	3.57 (1.17 L_{BP})	3.21 (1.05 L_{BP})	2.24 (0.73 L_{BP})	0.94 (0.31 L_{BP})	-	4.82 (1.58 L_{BP})
Time for yaw 90° (s)	19.84	22.47	24.56	29.42	-	19.64
Tactical diameter (m)	-	-	-	-	-	-
Time for yaw 180° (s)	-	-	-	-	-	-

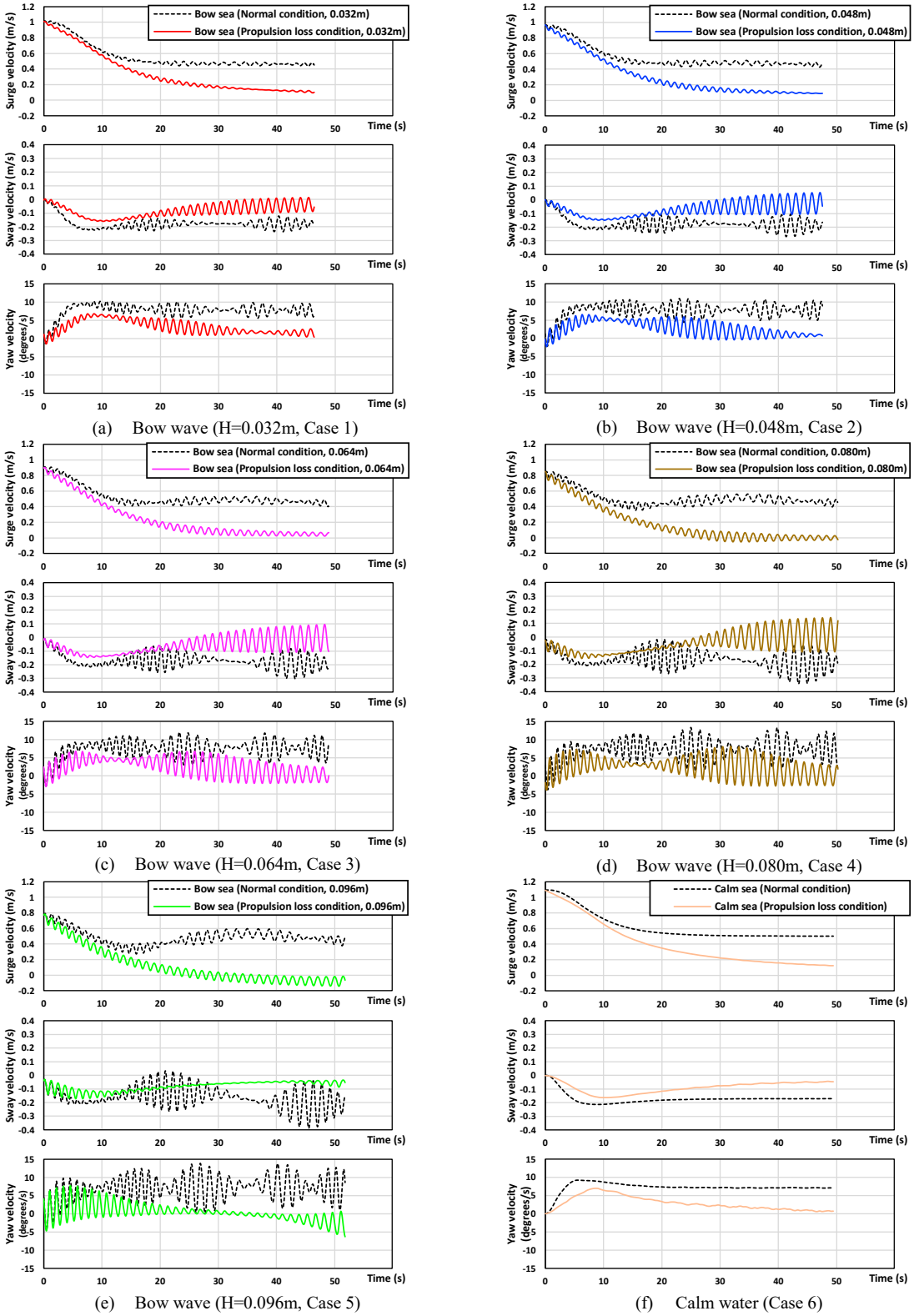

Fig. 6. The time histories of the ship velocities during the turning manoeuvre.

4. Conclusions and discussion

In the present study, the contribution of propulsion loss to the turning performance of the KCS under various wave height conditions was investigated by means of an unsteady RANS solver. Given scarce research on this topic, it is highly believed that the results obtained from this work would be helpful for Master Mariners and navigating officers to have a practical insight into the manoeuvring performance of the ship suffering from the propulsion loss condition, contributing to the development of standards for navigational safety in a real seaway. The key findings of this study can be summarised as follows:

- The loss of propulsion power caused substantial changes in the turning trajectories when compared to those experienced by the ship in the normal operating conditions, mainly due to the insufficient rudder normal force.
- It is important to highlight that the ship suffering from the propulsion failure condition could not complete the turning circle manoeuvre for all cases considered in this study, demonstrating the poor turning capability of the ship.
- It was clearly observed that the propulsion loss noticeably affected the speed loss during the turning manoeuvre when compared to that experienced by the turning ship under the normal conditions, leading to significant changes in the critical turning indices.

Proposed future work should undertake a more comprehensive analysis considering various external disturbances (such as irregular waves, currents, and winds) with particular attention to path-following and turning manoeuvres.

Acknowledgements

Results were obtained using the ARCHIE-WeSt High Performance Computer (www.archie-west.ac.uk) based at the University of Strathclyde. The authors gratefully acknowledge that the research presented in this paper was carried out as part of the EU funded H2020 project, VENTuRE (grant no. 856887).

References

Broglia, R., Dubbioso, G., Durante, D., Di Mascio, A., 2015. Turning ability analysis of a fully appended twin screw vessel by CFD. Part I: Single rudder configuration. Ocean Engineering 105, 275-286.

EMSA, 2021. Annual Overview of Marine Casualties and Incidents 2021.

Hasnan, M., Yasukawa, H., Hirata, N., Terada, D., Matsuda, A., 2019. Study of ship turning in irregular waves. Journal of Marine Science and Technology, 1-20.

ITTC, 2021. The Manoeuvring Committee Final Report and Recommendations to the 29th ITTC.

Kim, D., Song, S., Jeong, B., Tezdogan, T., 2021a. Numerical evaluation of a ship's manoeuvrability and course keeping control under various wave conditions using CFD. Ocean Engineering 237, 109615.

Kim, D., Song, S., Jeong, B., Tezdogan, T., Incecik, A., 2021b. Unsteady RANS CFD simulations of ship manoeuvrability and course keeping control under various wave height conditions. Applied Ocean Research 117, 102940.

Kim, D., Song, S., Sant, T., Demirel, Y.K., Tezdogan, T., 2022. Nonlinear URANS model for evaluating course keeping and turning capabilities of a vessel with propulsion system failure in waves. International journal of naval architecture and ocean engineering 14, 100425.

Kim, D., Song, S., Tezdogan, T., 2021c. Free running CFD simulations to investigate ship manoeuvrability in waves. Ocean Engineering 236, 109567.

Kim, D., Tezdogan, T., 2022. CFD-based hydrodynamic analyses of ship course keeping control and turning performance in irregular waves. Ocean Engineering 248, 110808.

Kim, I.-T., Kim, C., Kim, S.-H., Ko, D., Moon, S.-H., Park, H., Kwon, J., Jin, B., 2021d. Estimation of the manoeuvrability of the KVLCC2 in calm water using free running simulation based on CFD. International journal of naval architecture and ocean engineering.

Menter, F.R., 1994. Two-equation eddy-viscosity turbulence models for engineering applications. AIAA journal 32 (8), 1598-1605.

Terziev, M., Tezdogan, T., Incecik, A., 2020. Application of eddy-viscosity turbulence models to problems in ship hydrodynamics. Ships and Offshore Structures 15 (5), 511-534.

Wang, J., Zhao, W., Wan, D., 2016. Free maneuvering simulation of ONR Tumblehome using overset grid method in naoe-FOAM-SJTU solver, 31th Symposium on Naval Hydrodynamics, Monterey, USA.